Published for SISSA by Springer

Received: *July 22, 2025*
Accepted: *November 19, 2025*
Published: *December 19, 2025*

Measurement of the $B^0 \to \rho(770)^0\gamma$ branching fraction

The LHCb collaboration

E-mail: odescham@in2p3.fr

Abstract: The ratio between the branching fractions of the $B^0 \to \rho(770)^0\gamma$ and $B^0 \to K^*(892)^0\gamma$ decays is measured with proton-proton collision data collected by the LHCb experiment at centre-of-mass energies of 7, 8, and 13 TeV, corresponding to an integrated luminosity of 9 fb^{-1}. The measured value is

$$\frac{\mathcal{B}(B^0 \to \rho(770)^0\gamma)}{\mathcal{B}(B^0 \to K^*(892)^0\gamma)} = 0.0189 \pm 0.0007 \pm 0.0005,$$

where the first uncertainty is statistical and the second systematic. The branching fraction for $B^0 \to \rho(770)^0\gamma$ decays is hence obtained as

$$\mathcal{B}(B^0 \to \rho(770)^0\gamma) = (7.9 \pm 0.3 \pm 0.2 \pm 0.2) \times 10^{-7},$$

where the last uncertainty is due to the branching fraction of the normalisation mode. This result assumes that both the $\rho(770)^0$ and $K^*(892)^0$ decays saturate the dihadron mass spectra considered in the analysis. It is consistent with the current world-average value and by far the most precise measurement to date.

Keywords: B Physics, Flavour Physics, Hadron-Hadron Scattering, Rare Decay

ArXiv ePrint: 2507.14401

https://doi.org/10.1007/JHEP12(2025)151

JHEP12(2025)151

Contents

1 Introduction

In the Standard Model of particle physics (SM), the $b \to d\gamma$ and $b \to s\gamma$ flavour-changing neutral transitions proceed at leading order through electroweak loop (penguin) diagrams involving virtual W bosons and up-type quarks. The virtual contribution of the top quark is dominant due to its large mass, implying these processes mostly depend on the Cabibbo-Kobayashi-Maskawa (CKM) matrix elements V_{td} and V_{ts}, respectively. Extensions of the SM predict additional contributions that can significantly affect the dynamics of flavour-changing neutral transitions [1–3].

The suppressed $b \to d\gamma$ transition is an important but relatively unexplored probe of the SM. The transition was first observed in 2008 through the $B^0 \to \rho^0\gamma$ decay[1] by both Belle [4] and BaBar [5] experiments. A recent combination, including the Belle II measurement [6], gives a branching fraction of $\mathcal{B}(B^0 \to \rho^0\gamma) = (8.2 \pm 1.3) \times 10^{-7}$ [7]. The isospin-companion decay, $B^+ \to \rho^+\gamma$,[2] is measured with a similar decay rate, $\mathcal{B}(B^+ \to \rho^+\gamma) = (9.8 \pm 2.5) \times 10^{-7}$ [8]. Evidence for the $B^0 \to \omega\gamma$ decay was also reported by the Belle and BaBar experiments, with a combined branching fraction of $\mathcal{B}(B^0 \to \omega\gamma) = (4.4^{+1.8}_{-1.6}) \times 10^{-7}$ [8].

A precise measurement of the branching fraction ratio $\mathcal{B}(B^0 \to \rho^0\gamma)/\mathcal{B}(B^0 \to K^{*0}\gamma)$[3] could in principle provide an independent and direct constraint on the ratio of the CKM matrix elements $|V_{td}/V_{ts}|$, whose precision is limited by the theoretical inputs in the interpretation of the oscillation frequencies of the neutral B^0 and B^0_s mesons [8]. Currently, the constraint from radiative decays suffers from even larger theoretical uncertainties arising from the calculation of the hadronic $B^0 \to \rho^0$ and $B^0 \to K^{*0}$ form factors [9, 10]. Further advancements in the form-factor calculations will be crucial to derive a competitive constraint on the ratio $|V_{td}/V_{ts}|$ from the measured branching fractions of radiative decays.

[1]The symbol ρ^0 is used to refer to the $\rho(770)^0$ meson throughout the paper.
[2]The inclusion of charge-conjugate processes is implied throughout.
[3]The symbol K^{*0} is used to refer to the $K^*(892)^0$ meson throughout the paper.

JHEP12(2025)151

In this paper, the branching fraction of the $B^0 \to \rho^0\gamma$ decay is measured with respect to the normalisation channel, $B^0 \to K^{*0}\gamma$, using the resonance decays $\rho^0 \to \pi^+\pi^-$ and $K^{*0} \to K^+\pi^-$, respectively. This is the first measurement related to the $b \to d\gamma$ transition performed by LHCb. Both decay modes share a similar final-state topology allowing for the cancellation of most of the systematic uncertainties related to the recorded luminosity, the decay reconstruction and the selection efficiencies. The ratio of branching fractions is measured as

$$\frac{\mathcal{B}(B^0 \to \rho^0\gamma)}{\mathcal{B}(B^0 \to K^{*0}\gamma)} = \frac{N(B^0 \to \rho^0(\pi^+\pi^-)\gamma)}{N(B^0 \to K^{*0}(K^+\pi^-)\gamma)} \times \frac{\varepsilon(B^0 \to K^{*0}(K^+\pi^-)\gamma)}{\varepsilon(B^0 \to \rho^0(\pi^+\pi^-)\gamma)} \times \mathcal{R}_{\mathcal{B}}, \tag{1.1}$$

where N and ε respectively stand for the measured yield and the overall selection efficiency of the $B^0 \to \rho^0(\pi^+\pi^-)\gamma$ and $B^0 \to K^{*0}(K^+\pi^-)\gamma$ samples. The last term, $\mathcal{R}_{\mathcal{B}} = \mathcal{B}(K^{*0} \to K^+\pi^-)/\mathcal{B}(\rho^0 \to \pi^+\pi^-)$, represents the ratio of the $K^{*0} \to K^+\pi^-$ and $\rho^0 \to \pi^+\pi^-$ decay rates.

The analysis uses the Run 1 (2011–2012) and Run 2 (2015–2018) LHCb data samples of proton-proton (pp) collisions at centre-of-mass energies of 7 TeV (2011), 8 TeV (2012), and 13 TeV (Run 2), corresponding to an integrated luminosity of about 9 fb^{-1}. To avoid experimenter's bias, the candidates in the signal region, corresponding to an invariant mass of $m(\pi^+\pi^-\gamma) \in [5150, 5490]$ MeV/c^2, were not examined until the selection and analysis procedures are finalised. The studies were done separately per data-taking period to account for possible variations of the experimental conditions, and merged at the last step of the analysis.

2 Detector and simulation

The LHCb detector [11, 12] is a single-arm forward spectrometer covering the pseudorapidity range $2 < \eta < 5$, designed for the study of particles containing b or c quarks. The detector used for this analysis includes a high-precision tracking system consisting of a silicon-strip vertex detector surrounding the pp interaction region [13], a large-area silicon-strip detector located upstream of a dipole magnet with a bending power of about 4 T m, and three stations of silicon-strip detectors and straw drift tubes [14, 15] placed downstream of the magnet. The tracking system provides a measurement of the momentum, p, of charged particles with a relative uncertainty that varies from 0.5% at low momentum to 1.0% at 200 GeV/c. The minimum distance of a track to a primary pp collision vertex (PV), the impact parameter (IP), is measured with a resolution of $(15+29/p_{\mathrm{T}})$ μm, where p_{T} is the component of the momentum transverse to the beam, in GeV/c. Different types of charged hadrons are distinguished using information from two ring-imaging Cherenkov detectors (RICH) [16]. Photons, electrons and hadrons are identified by a calorimeter system consisting of scintillating-pad and preshower detectors, an electromagnetic (ECAL) and a hadronic calorimeter. Muons are identified by a system composed of alternating layers of iron and multiwire proportional chambers [17].

Simulated events are used to optimise the signal selection and to parameterise the reconstructed invariant-mass distributions for the B^0 meson. Contributions from specific background channels are also studied using dedicated simulation samples. In the simulation, pp collisions are generated using PYTHIA [18, 19] with a specific LHCb configuration [20]. The decay chain of hadronic particles and the final-state radiation are handled by EVTGEN [21] and

PHOTOS [22], respectively. The detector response to the interacting particles is implemented in the GEANT4 toolkit [23, 24].

3 Event selection

The online event selection is performed by a trigger [25, 26], which consists of a hardware stage, based on information from the calorimeter and muon systems, followed by a software stage, which applies the full event reconstruction. The hardware trigger selects events having an ECAL cluster with an energy component transverse to the beam (E_{T}) above a threshold of 2.50 GeV and 2.96 GeV in Run 1 and Run 2, respectively. The software trigger requires two high-p_{T} hadrons significantly displaced from the interaction point, and one high-E_{T} photon [27]. The trigger efficiency is further enhanced by about 20% by applying loose track-selection requirements to events that pass a tight photon threshold of $E_{\mathrm{T}} > 4\,\mathrm{GeV}$ at the hardware stage. For Run 2 data, a multivariate classifier based on topological criteria complements the cut-based software trigger selection [28].

The reconstructed B^0 candidate combines a pair of good-quality tracks [29] and an energetic photon. The two charged tracks are required to have large IP, with a significance with respect to any PV [30] greater than four. Both tracks must have a p_{T} larger than $500\,\mathrm{MeV}/c$ with at least one above $1.2\,\mathrm{GeV}/c$. To reduce the background from partially reconstructed B decays, the B^0 decay vertex is required to be isolated applying a lower limit on the $\Delta\chi^2_{\mathrm{vtx}}(B^0)$ variable, defined as the increase in the vertex fit χ^2 when adding any additional reconstructed track.

Photon candidates are identified from ECAL clusters that cannot be geometrically associated with any extrapolated track. The photon four-momentum is evaluated using the dihadron vertex as the origin and the position and energy of the associated cluster. The transverse component of the reconstructed photon momentum is required to be larger than $3\,\mathrm{GeV}/c$. The B^0 candidate four-momentum is computed by summing the four-momenta of the two hadrons and the photon. The B^0 momentum is required to point back to the associated primary vertex and to have a transverse component larger than $2\,\mathrm{GeV}/c$. The B^0 candidates are selected in the mass range $[4000, 7000]\,\mathrm{MeV}/c^2$. The reconstructed mass of the $\pi^+\pi^-$ pair must fall within $[630, 920]\,\mathrm{MeV}/c^2$ and the $K^+\pi^-$ mass within $[795.5, 995.5]\,\mathrm{MeV}/c^2$.

For the $B^0 \to \rho^0(\pi^+\pi^-)\gamma$ channel, charged hadrons are identified as pions using information provided by the RICH system. The probability associated to the pion hypothesis must be larger than any other hadron hypothesis, kaon or proton, and larger than a threshold optimised to reduce the expected contamination due to decays of b hadrons with a similar topology. The optimisation is done by maximising the ratio $S/\sqrt{S + \sum_i B_i}$ where S stands for the expected signal yield, based on the known $B^0 \to \rho^0\gamma$ branching fraction [8], and B_i are the expected background yields for $B^0 \to K^{*0}(K^+\pi^-)\gamma$, $B^0_s \to \phi(K^+K^-)\gamma$ and $\Lambda^0_b \to pK^-\gamma$ decays. This optimisation is performed for each year of data-taking using simulated samples and deriving particle-identification (PID) performance from dedicated calibration-data samples. Fiducial ranges for track momentum, $p \in [4.5, 100.0]\,\mathrm{GeV}/c$, and pseudorapidity, $\eta \in [1.5, 4.5]$, are applied to match the phase space covered by the data-driven calibration tool [31]. The charged-particle PID efficiency for the $B^0 \to \rho^0(\pi^+\pi^-)\gamma$ channel, corresponding to the probability that both pions are correctly identified, is about 70%. In contrast, the

JHEP12(2025)151

PID efficiency for the $B^0 \to K^{*0}(K^+\pi^-)\gamma$ channel, where the kaon is misidentified as a pion, is around 0.5%. For the $B^0 \to K^{*0}(K^+\pi^-)\gamma$ normalisation channel, the hadron-identification criteria were optimised in a previous radiative decay analysis [32], which uses the same procedure as that described here.

Regarding the photon identification, the main background comes from $\pi^0 \to \gamma\gamma$ decays for which the pair of photons form a single ECAL cluster. Single photons and neutral pions are distinguished by exploiting their cluster shape and energy distribution, using a dedicated tool [33]. The optimisation of the photon-identification criteria is performed with respect to the $B^0 \to \rho^0(\pi^+\pi^-)\pi^0$ decay mode. Given that its branching fraction is measured with a large relative uncertainty of 25%, the photon-identification criteria are obtained by minimising the expected relative uncertainty on the $B^0 \to \rho^0(\pi^+\pi^-)\gamma$ measured yield, accounting for the $B^0 \to \rho^0(\pi^+\pi^-)\pi^0$ contamination and its uncertainty. As for charged-particle identification, the optimisation is performed for each year of data-taking using simulated samples and deriving PID performance from dedicated calibration-data samples. Other contributions from $B^0 \to (\pi^\pm\pi^0)h^\mp$ decays, where h stands for a pion or a kaon, that involve a $(\pi^\pm\pi^0)$ resonant state, including charmed $D^\pm$ meson decays, are vetoed by requiring that the invariant mass of the reconstructed $\pi^\pm\gamma$ system $(m_{\pi^\pm\gamma})$, where the neutral pion mass is assigned to the reconstructed photon, exceeds $2\,\mathrm{GeV}/c^2$. This criterion, referred to as the charm veto, also suppresses contributions from charmless $B^0 \to \rho^\pm\pi^\mp$ and $B^0 \to K^{*\pm}\pi^\mp$ decays and backgrounds from partially reconstructed B decays involving misidentified π^0 mesons. Both the photon-identification criteria and the charm veto are consistently applied to the $K^+\pi^-\gamma$ sample selection.

Background candidates resulting from combinations of unrelated hadrons and photons, denoted as combinatorial background, can be strongly suppressed by exploiting kinematic and topological variables. Boosted decision tree (BDT) classifiers [34, 35] are trained for each year of data taking using simulated events, matched to the detector conditions, as signal proxy and data candidates selected with $m_{\pi^+\pi^-\gamma} > m_{B^0} + 300\,\mathrm{MeV}/c^2$ as background proxy, where m_{B^0} is the known B^0 mass [8]. An extended dipion mass range, $m_{\pi^+\pi^-} < 1500\,\mathrm{MeV}/c^2$, is applied to increase the number of $\pi^+\pi^-\gamma$ candidates available for the training. The input variables to the classifier are the IP and the p_T of each hadron candidate and of the dihadron combination, as well as the momentum, pseudorapidity, flight distance, IP significance and $\Delta\chi^2_\mathrm{vtx}(B^0)$ of the reconstructed B^0 candidate. In Run 2, the BDT also makes use of the cone isolation variable defined as

$$I_{p_\mathrm{T}} = \frac{p_\mathrm{T}(B^0) - \sum p_\mathrm{T}}{p_\mathrm{T}(B^0) + \sum p_\mathrm{T}}, \tag{3.1}$$

where the sum is taken over tracks that are not part of the B^0 signal candidate but are associated with the same PV and fall within a cone of half-angle $\Delta R_c = 1.7\,\mathrm{rad}$, $\Delta R < \Delta R_c$. The track ΔR is evaluated according to $(\Delta R)^2 = (\Delta\theta)^2 + (\Delta\phi)^2$, where $\Delta\theta$ and $\Delta\phi$ are the differences in the polar and azimuthal angles of the track momentum with respect to the direction of the B^0 candidate. A two-sample cross-validation technique is used to avoid overfitting the BDT model. A separate BDT algorithm with the same configuration and input variables is similarly trained to select $B^0 \to K^{*0}(K^+\pi^-)\gamma$ candidates.

JHEP12(2025)151

Before training the BDT, weights are applied to the simulated candidates to correct for imperfections in the simulation of kinematic variables. They are obtained by comparing simulated and background-subtracted data distributions for $B^0 \to K^{*0}(K^+\pi^-)\gamma$, applying all the $K^+\pi^-\gamma$ selection criteria except the BDT itself, and using the sPlot technique [36]. A gradient-BDT reweighter [37] is trained on the number of tracks per event, the momentum and pseudorapidity of the B^0 candidate, the transverse momenta of the photon and the dihadron candidates and, for Run 2, the cone isolation variable $I_{p_{\mathrm{T}}}$. The derived weights are applied to both the $B^0 \to \rho^0(\pi^+\pi^-)\gamma$ and $B^0 \to K^{*0}(K^+\pi^-)\gamma$ simulated candidates. An overall good agreement between data and simulation is obtained in the distributions of the variables used to train the BDT. The effects of remaining discrepancies are considered as systematic uncertainties by using alternative weighting schemes.

The BDT working points are optimised for each year of data-taking by maximising the ratio $S/\sqrt{S+B}$, where S is the expected number of signal candidates estimated from simulation and B is the number of combinatorial background candidates in the signal region estimated by extrapolating the data distribution in the upper mass sideband of the signal peak.

After the selection, in the $K^+\pi^-\gamma$ sample, the expected contributions of the dominant backgrounds, relative to the $B^0 \to K^{*0}(K^+\pi^-)\gamma$ normalisation yield, are as follows: 0.4% from $B_s^0 \to \phi(K^+K^-)\gamma$, 0.5% from $\Lambda_b^0 \to pK^-\gamma$ and 1.6% from $B^0 \to K^+\pi^-\pi^0$ for which one of the particles is misidentified; 0.8% from the suppressed $\overline{B}_s^0 \to K^{*0}(K^+\pi^-)\gamma$ mode; and 1.6% from $B^0 \to K^{*0}(K^+\pi^-)\eta(\gamma\gamma)$ for which one of the photons is not reconstructed. Similarly, in the $\pi^+\pi^-\gamma$ sample, the expected background contributions, relative to the $B^0 \to \rho^0(\pi^+\pi^-)\gamma$ signal yield, are as follows: 11% from $B^0 \to K^{*0}(K^+\pi^-)\gamma$ and 12% from $B^0 \to \rho^0(\pi^+\pi^-)\pi^0$ for which one particle is misidentified; 0.4% from $B^0 \to K^+\pi^-\pi^0$ where both the kaon and the neutral pion are misidentified; 13% from $B_s^0 \to \phi(\pi^+\pi^-\pi^0)\gamma$ for which the neutral pion escapes reconstruction; and 0.9% from $B^0 \to \rho^0(\pi^+\pi^-)\eta(\gamma\gamma)$ for which one of the photons is not reconstructed. For both samples, the $B^0 \to K^+\pi^-\pi^0$ decay is simulated using an amplitude model derived from ref. [38].

4 Invariant-mass fit

A simultaneous unbinned maximum-likelihood fit to the $K^+\pi^-\gamma$ and $\pi^+\pi^-\gamma$ invariant-mass distributions is performed in the range $[5010, 6410]\,\mathrm{MeV}/c^2$ to determine the yields of the signal and normalisation modes, combining the Run 1 and Run 2 data samples. The invariant-mass distributions of the $B^0 \to \rho^0(\pi^+\pi^-)\gamma$ and $B^0 \to K^{*0}(K^+\pi^-)\gamma$ components are modelled using a modified double-sided Crystal Ball (ADSCB) [39] probability density function (PDF) with an asymmetrical Gaussian core and tails on both sides. The mean, the width of the Gaussian core, and the right-tail threshold parameters are shared between the signal and the normalisation modes and are allowed to float in the fit. The right-tail power parameter and the two left-tail parameters are fixed separately for each mode to the values obtained from fits to simulation samples.

For both the $\pi^+\pi^-\gamma$ and $K^+\pi^-\gamma$ mass distributions, the shapes of the combinatorial backgrounds are modelled using first-order polynomial functions with slopes and yields allowed to vary in the fit. The backgrounds arising from partially reconstructed B decays are modelled with an Argus [40] function convolved with the experimental signal resolution.

Source	Uncertainty [%]
Signal mass model	(+0.5, −0.6)
Background contributions	(+2.0, −2.2)
Background mass models	(+1.1, −0.8)
Total systematic uncertainty	(+2.3, −2.4)

Table 1. Relative systematic uncertainties on the measured yield ratio for the different sources described in the text.

The slopes of the Argus functions are fixed to their values determined from simulation. The missing-mass parameters of the Argus functions are fixed to the mass of the π^0 meson. The power parameters and the yields are free to vary in the fit to accommodate the limited knowledge of the contributions to these missing pion components.

Specific background modes, listed at the end of the previous section, are included as individual components in the fit models. Their shapes are described with either ADSCB or Argus functions with all parameters fixed to the values obtained from simulation. Their individual contributions, to either the $K^+\pi^-\gamma$ or $\pi^+\pi^-\gamma$ data samples, are made independent of the measured $B^0 \to \rho^0(\pi^+\pi^-)\gamma$ signal yield by defining all of them as a fixed fraction of the fitted $B^0 \to K^{*0}(K^+\pi^-)\gamma$ normalisation yield.

The resulting invariant-mass fit is displayed in figure 1. The obtained $B^0 \to \rho^0(\pi^+\pi^-)\gamma$ signal and $B^0 \to K^{*0}(K^+\pi^-)\gamma$ normalisation yields are $1\,917 \pm 71$ and $148\,160 \pm 900$, respectively, where the uncertainties are statistical only. The yield ratio is measured to be

$$\frac{N(B^0 \to \rho^0(\pi^+\pi^-)\gamma)}{N(B^0 \to K^{*0}(K^+\pi^-)\gamma)} = 0.0129 \pm 0.0005 \pm 0.0003,$$

where the first uncertainty is statistical and the second is the overall systematic uncertainty resulting from the individual contributions listed in table 1 and summarised below. Conservatively, individual sources are added in quadrature for the positive and negative components separately.

The uncertainty due to the fixed tail parameters in the signal model is determined using pseudoexperiments. The data fit is repeated 1000 times, with the value of the tail parameters sampled according to a multidimensional Gaussian PDF based on the covariance matrix obtained from a simultaneous fit to the $B^0 \to \rho^0(\pi^+\pi^-)\gamma$ and $B^0 \to K^{*0}(K^+\pi^-)\gamma$ simulated samples. Additionally, a potential difference in the invariant-mass resolution between signal and normalisation modes is investigated by introducing scale factors on the associated parameters. By adding in quadrature the systematic uncertainties related to the signal mass model, a relative uncertainty of $\left(^{+0.5}_{-0.6}\right)\%$ is obtained on the yield ratio.

The specific background contributions are fixed in the simultaneous fit to the two data samples. The associated uncertainties are obtained using pseudoexperiments where each individual contribution is varied within its uncertainty. The resulting uncertainty on the yield ratio is found to be $\left(^{+2.0}_{-2.2}\right)\%$, primarily due to the limited knowledge of the branching fraction of the $B^0 \to \rho^0(\pi^+\pi^-)\pi^0$ decay mode. Regarding the description of the background mass models, the associated uncertainties are determined by varying the fixed parameters

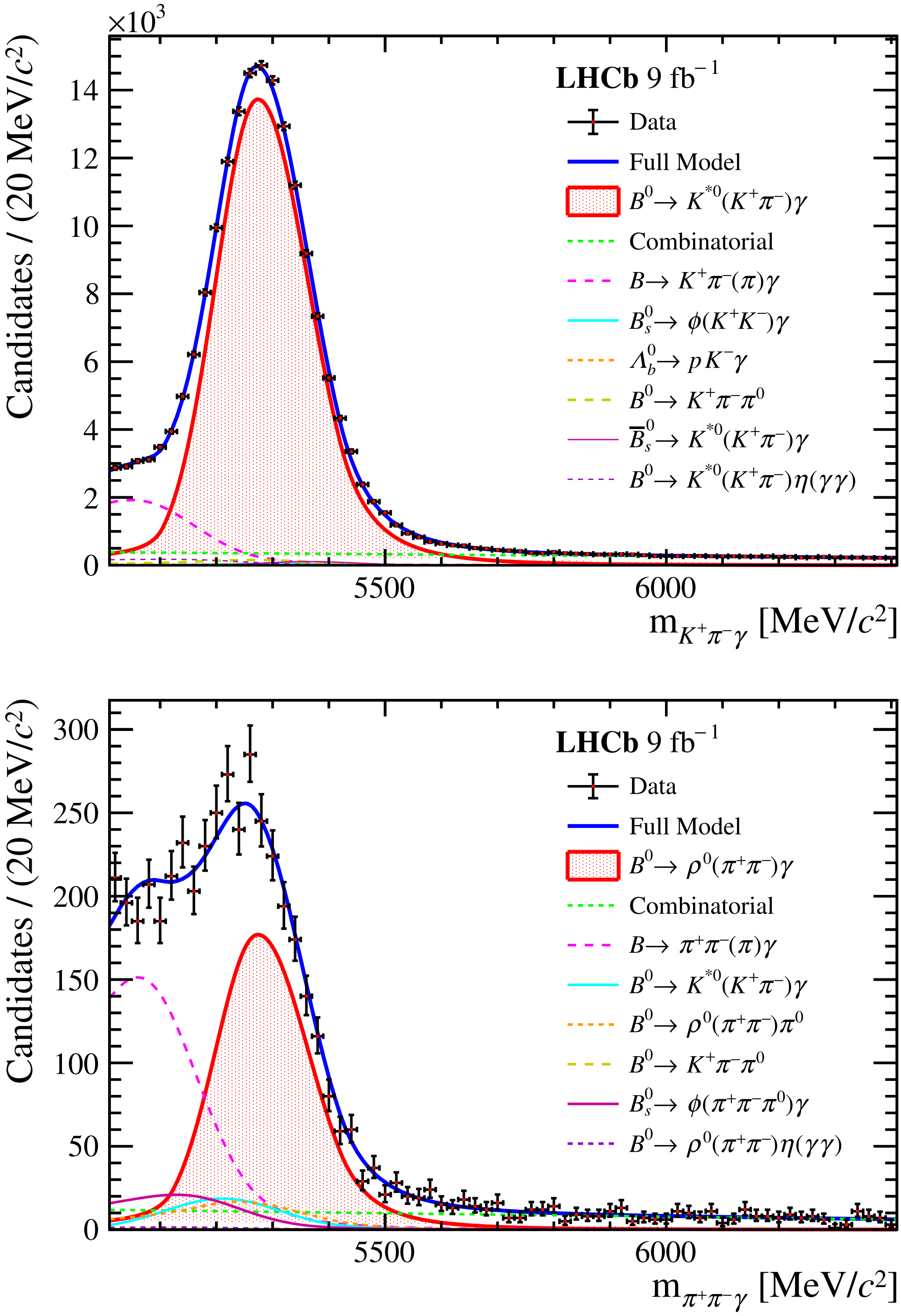

Figure 1. Invariant-mass distribution for the (top) $K^+\pi^-\gamma$ and (bottom) $\pi^+\pi^-\gamma$ selected candidates in the dihadron mass range $m_{K^+\pi^-} \in [795.5, 995.5]\,\mathrm{MeV}/c^2$ and $m_{\pi^+\pi^-} \in [630, 920]\,\mathrm{MeV}/c^2$, respectively, combining Run 1 and Run 2 data samples. The fit components are also shown.

JHEP12(2025)151

in the respective PDFs within their uncertainties, or by using alternative models. Summing all the background-model sources in quadrature, an overall uncertainty of $\left(^{+1.1}_{-0.8}\right)\%$ on the yield ratio is obtained.

The invariant-mass fit is also repeated with the lower bound of the fitted mass range extended to $4700\,\mathrm{MeV}/c^2$ both for the signal and normalisation channels. Partially reconstructed B decays with two or more missing pions, which populate this lower mass region are included as an additional component modelled with an Argus function convolved with the signal resolution. The missing-mass parameter of the Argus function is fixed to twice the mass of the π^0 meson. For each of the two samples, the Argus power parameter and the associated yield are allowed to vary freely. The obtained yield ratio is found to be compatible with the nominal fit, and no additional uncertainty is assigned.

5 Efficiency ratio

The overall efficiency to reconstruct and select the signal and normalisation decays is factorised as

$$\varepsilon = \varepsilon_{\mathrm{sel}} \times \varepsilon^{h^\pm}_{\mathrm{PID}} \times \varepsilon^{\gamma}_{\mathrm{PID}}. \tag{5.1}$$

The term $\varepsilon_{\mathrm{sel}}$, obtained from simulations, includes the geometrical acceptance of the spectrometer, the efficiency of the trigger requirements, and the different stages of the selection except PID criteria. In particular, the efficiencies related to the $K^+\pi^-$ and $\pi^+\pi^-$ mass-window selections are accounted for. A relative uncertainty of $\pm 0.8\%$ on the efficiency ratio, $\varepsilon(B^0 \to K^{*0}(K^+\pi^-)\gamma)/\varepsilon(B^0 \to \rho^0(\pi^+\pi^-)\gamma)$, is assigned owing to the limited size of the simulated samples. Alternative weighting corrections are tested for the kinematic distributions of the simulated samples, resulting in a systematic uncertainty of $\left(^{+1.1}_{-0.2}\right)\%$ on the efficiency ratio. Differences between kaon and pion reconstruction efficiencies lead to an additional $\pm 0.3\%$ uncertainty.

The efficiencies related to the identification of the charged hadrons $\varepsilon^{h^\pm}_{\mathrm{PID}}$ are measured using high-purity calibration samples of $D^{*+} \to D^0(K^-\pi^+)\pi^+$ decays, and are evaluated as a function of the hadron momentum and pseudorapidity using a dedicated procedure [31]. The overall uncertainty on the efficiency ratio, which includes the effect of the limited size of the calibration samples, the correlation between the two final-state hadrons and limitations of the procedure, is estimated to be $\left(^{+0.7}_{-1.3}\right)\%$. The photon-identification efficiency $\varepsilon^{\gamma}_{\mathrm{PID}}$ is estimated from a reference data sample using a similar method [33]. The associated uncertainties mostly cancel in the efficiency ratio between the two radiative modes resulting in a systematic effect estimated as $\pm 0.1\%$.

The ratio of efficiencies, obtained from a year-weighted average, is determined to be

$$\frac{\varepsilon(B^0 \to K^{*0}(K^+\pi^-)\gamma)}{\varepsilon(B^0 \to \rho^0(\pi^+\pi^-)\gamma)} = 2.20 \pm 0.02 \pm 0.03,$$

where the first uncertainty is statistical and the second systematic, resulting from the quadratic sum of the individual contributions summarised in table 2. The value of the efficiency ratio is explained by a more stringent selection for the $B^0 \to \rho^0\gamma$ channel.

JHEP12(2025)151

Source	Uncertainty [%]
Simulated samples size	(+0.8, −0.8)
Kinematics corrections	(+1.1, −0.2)
Kaon/pion reconstruction	(+0.3, −0.3)
Charged PID	(+0.7, −1.3)
Neutral PID	(+0.1, −0.1)
Total systematic uncertainty	(+1.6, −1.6)

Table 2. Relative systematic uncertainties on the efficiency ratio for the different sources described in the text.

6 Results

Using the known branching fraction of K^{*0} decays into $K^+\pi^-$ [8], and neglecting any suppressed decay of the ρ^0 meson, the ratio of decay rates $\mathcal{R}_b$ is taken as $\mathcal{B}(K^{*0} \to K^+\pi^-) = (66.507 \pm 0.014)\%$, which gives a ratio of branching fractions

$$\frac{\mathcal{B}(B^0 \to \rho^0\gamma)}{\mathcal{B}(B^0 \to K^{*0}\gamma)} = 0.0189 \pm 0.0007 \pm 0.0005,$$

where the first uncertainty is statistical and the second systematic. The uncertainty on the $K^{*0} \to K^+\pi^-$ branching fraction is negligible.

Combining this with the known branching fraction for the $B^0 \to K^{*0}\gamma$ decay [7], the branching fraction is determined to be

$$\mathcal{B}(B^0 \to \rho^0\gamma) = (7.9 \pm 0.3 \pm 0.2 \pm 0.2) \times 10^{-7},$$

where the last uncertainty is due to the branching fraction of the normalisation mode. The measured branching fraction is in good agreement with the current world average and is by far the most precise to date [7].

The analysis of the $B^0 \to \rho^0(\pi^+\pi^-)\gamma$ decay presented here uses candidates in the dipion invariant-mass range $[630, 920]\,\mathrm{MeV}/c^2$ assuming that the $\rho^0 \to \pi^+\pi^-$ decay saturates the dipion spectrum in this range. The small contribution from $\omega \to \pi^+\pi^-$ decay and any possible contribution from wide resonances at higher mass are neglected. Similarly, the analysis of the $B^0 \to K^{*0}(K^+\pi^-)\gamma$ decay assumes that the K^{*0} decay saturates the $K^+\pi^-$ invariant-mass range $[795.5, 995.5]\,\mathrm{MeV}/c^2$ considered in this study. S-wave amplitudes are forbidden in radiative B^0 decays and nonresonant contributions with higher angular momentum are assumed to be negligible for both final states. Detailed amplitude analyses over wider dihadron invariant-mass ranges would provide better constraints on the resonant ρ^0 and K^{*0} contributions to the respective radiative decays.

Acknowledgments

We express our gratitude to our colleagues in the CERN accelerator departments for the excellent performance of the LHC. We thank the technical and administrative staff at the

LHCb institutes. We acknowledge support from CERN and from the national agencies: ARC (Australia); CAPES, CNPq, FAPERJ and FINEP (Brazil); MOST and NSFC (China); CNRS/IN2P3 (France); BMBF, DFG and MPG (Germany); INFN (Italy); NWO (Netherlands); MNiSW and NCN (Poland); MCID/IFA (Romania); MICIU and AEI (Spain); SNSF and SER (Switzerland); NASU (Ukraine); STFC (United Kingdom); DOE NP and NSF (U.S.A.). We acknowledge the computing resources that are provided by ARDC (Australia), CBPF (Brazil), CERN, IHEP and LZU (China), IN2P3 (France), KIT and DESY (Germany), INFN (Italy), SURF (Netherlands), Polish WLCG (Poland), IFIN-HH (Romania), PIC (Spain), CSCS (Switzerland), and GridPP (United Kingdom). We are indebted to the communities behind the multiple open-source software packages on which we depend. Individual groups or members have received support from Key Research Program of Frontier Sciences of CAS, CAS PIFI, CAS CCEPP, Fundamental Research Funds for the Central Universities, and Sci. & Tech. Program of Guangzhou (China); Minciencias (Colombia); EPLANET, Marie Skłodowska-Curie Actions, ERC and NextGenerationEU (European Union); A*MIDEX, ANR, IPhU and Labex P2IO, and Région Auvergne-Rhône-Alpes (France); Alexander-von-Humboldt Foundation (Germany); ICSC (Italy); Severo Ochoa and María de Maeztu Units of Excellence, GVA, XuntaGal, GENCAT, InTalent-Inditex and Prog. Atracción Talento CM (Spain); SRC (Sweden); the Leverhulme Trust, the Royal Society and UKRI (United Kingdom).

Data Availability Statement. This article has no associated data or the data will not be deposited.

Code Availability Statement. This article has no associated code or the code will not be deposited.

References

[1] A. Arhrib, C.-K. Chua and W.-S. Hou, *Supersymmetric model contributions to $B_d^0 - \bar{B}_d^0$ mixing and $B \to \pi\pi$, $\rho\gamma$ decays*, Eur. Phys. J. C **21** (2001) 567 [hep-ph/0104122] [INSPIRE].

[2] A. Ali and E. Lunghi, *Implications of $B \to \rho\gamma$ measurements in the standard model and supersymmetric theories*, Eur. Phys. J. C **26** (2002) 195 [hep-ph/0206242] [INSPIRE].

[3] Z.-J. Xiao and C. Zhuang, *Exclusive $B \to (K^*, \rho)\gamma$ decays in the general two Higgs doublet models*, Eur. Phys. J. C **33** (2004) 349 [hep-ph/0310097] [INSPIRE].

[4] Belle collaboration, *Measurement of branching fractions, isospin and CP-violating asymmetries for exclusive $b \to d\gamma$ modes*, Phys. Rev. Lett. **101** (2008) 111801 [*Erratum ibid.* **101** (2008) 129904] [arXiv:0804.4770] [INSPIRE].

[5] BaBar collaboration, *Measurements of branching fractions for $B^+ \to \rho^+\gamma$, $B^0 \to \rho^0\gamma$, and $B^0 \to \omega\gamma$*, Phys. Rev. D **78** (2008) 112001 [arXiv:0808.1379] [INSPIRE].

[6] Belle and Belle-II collaborations, *Measurement of branching fractions, CP asymmetry, and isospin asymmetry for $B \to \rho\gamma$ decays using Belle and Belle II data*, Phys. Rev. D **111** (2025) L071103 [arXiv:2407.08984] [INSPIRE].

[7] Heavy Flavor Averaging Group (HFLAV) collaboration, *Averages of b-hadron, c-hadron, and τ-lepton properties as of 2023*, arXiv:2411.18639 [inSPIRE].

[8] Particle Data Group collaboration, *Review of particle physics*, *Phys. Rev. D* **110** (2024) 030001 [inSPIRE].

[9] P. Ball and R. Zwicky, *$|V_{td}/V_{ts}|$ from $B \to V\gamma$*, *JHEP* **04** (2006) 046 [hep-ph/0603232] [inSPIRE].

[10] P. Ball, G.W. Jones and R. Zwicky, *$B \to V\gamma$ beyond QCD factorisation*, *Phys. Rev. D* **75** (2007) 054004 [hep-ph/0612081] [inSPIRE].

[11] LHCb collaboration, *The LHCb detector at the LHC*, 2008 *JINST* **3** S08005 [inSPIRE].

[12] LHCb collaboration, *LHCb detector performance*, *Int. J. Mod. Phys. A* **30** (2015) 1530022 [arXiv:1412.6352] [inSPIRE].

[13] R. Aaij et al., *Performance of the LHCb vertex locator*, 2014 *JINST* **9** P09007 [arXiv:1405.7808] [inSPIRE].

[14] LHCb Outer Tracker Group collaboration, *Performance of the LHCb outer tracker*, 2014 *JINST* **9** P01002 [arXiv:1311.3893] [inSPIRE].

[15] LHCb Outer Tracker Group collaboration, *Improved performance of the LHCb outer tracker in LHC run 2*, 2017 *JINST* **12** P11016 [arXiv:1708.00819] [inSPIRE].

[16] LHCb RICH Group collaboration, *Performance of the LHCb RICH detector at the LHC*, *Eur. Phys. J. C* **73** (2013) 2431 [arXiv:1211.6759] [inSPIRE].

[17] A.A. Alves Jr. et al., *Performance of the LHCb muon system*, 2013 *JINST* **8** P02022 [arXiv:1211.1346] [inSPIRE].

[18] T. Sjöstrand, S. Mrenna and P.Z. Skands, *A brief introduction to PYTHIA 8.1*, *Comput. Phys. Commun.* **178** (2008) 852 [arXiv:0710.3820] [inSPIRE].

[19] T. Sjöstrand, S. Mrenna and P.Z. Skands, *PYTHIA 6.4 physics and manual*, *JHEP* **05** (2006) 026 [hep-ph/0603175] [inSPIRE].

[20] LHCb collaboration, *Handling of the generation of primary events in Gauss, the LHCb simulation framework*, *J. Phys. Conf. Ser.* **331** (2011) 032047 [inSPIRE].

[21] D.J. Lange, *The EvtGen particle decay simulation package*, *Nucl. Instrum. Meth. A* **462** (2001) 152 [inSPIRE].

[22] N. Davidson, T. Przedzinski and Z. Was, *PHOTOS interface in C++: technical and physics documentation*, *Comput. Phys. Commun.* **199** (2016) 86 [arXiv:1011.0937] [inSPIRE].

[23] J. Allison et al., *GEANT4 developments and applications*, *IEEE Trans. Nucl. Sci.* **53** (2006) 270 [inSPIRE].

[24] GEANT4 collaboration, *GEANT4 — a simulation toolkit*, *Nucl. Instrum. Meth. A* **506** (2003) 250 [inSPIRE].

[25] R. Aaij et al., *The LHCb trigger and its performance in 2011*, 2013 *JINST* **8** P04022 [arXiv:1211.3055] [inSPIRE].

[26] LHCb collaboration, *Design and performance of the LHCb trigger and full real-time reconstruction in run 2 of the LHC*, 2019 *JINST* **14** P04013 [arXiv:1812.10790] [inSPIRE].

[27] A. Puig, *The HLT2 radiative topological lines*, LHCb-PUB-2012-002, CERN, Geneva, Switzerland (2012) [inSPIRE].

[28] T. Likhomanenko et al., *LHCb topological trigger reoptimization*, *J. Phys. Conf. Ser.* **664** (2015) 082025 [arXiv:1510.00572] [INSPIRE].

[29] LHCb collaboration, *Measurement of the track reconstruction efficiency at LHCb*, 2015 *JINST* **10** P02007 [arXiv:1408.1251] [INSPIRE].

[30] M. Kucharczyk, P. Morawski and M. Witek, *Primary vertex reconstruction at LHCb*, LHCb-PUB-2014-044, CERN, Geneva, Switzerland (2014) [INSPIRE].

[31] L. Anderlini et al., *The PIDCalib package*, LHCb-PUB-2016-021, CERN, Geneva, Switzerland (2016) [INSPIRE].

[32] LHCb collaboration, *Amplitude analysis of the radiative decay* $B_s^0 \to K^+K^-\gamma$, *JHEP* **08** (2024) 093 [arXiv:2406.00235] [INSPIRE].

[33] M. Calvo Gomez et al., *A tool for* γ/π^0 *separation at high energies*, LHCb-PUB-2015-016, CERN, Geneva, Switzerland (2015).

[34] L. Breiman, J. Friedman, R.A. Olshen and C.J. Stone, *Classification and regression trees*, Chapman and Hall/CRC, U.S.A. (2017) [DOI:10.1201/9781315139470] [INSPIRE].

[35] Y. Freund and R.E. Schapire, *A decision-theoretic generalization of on-line learning and an application to boosting*, *J. Comput. Syst. Sci.* **55** (1997) 119 [INSPIRE].

[36] M. Pivk and F.R. Le Diberder, *SPlot: a statistical tool to unfold data distributions*, *Nucl. Instrum. Meth. A* **555** (2005) 356 [physics/0402083] [INSPIRE].

[37] A. Rogozhnikov, *Reweighting with boosted decision trees*, *J. Phys. Conf. Ser.* **762** (2016) 012036 [arXiv:1608.05806] [INSPIRE].

[38] BABAR collaboration, *Amplitude analysis of* $B^0 \to K^+\pi^-\pi^0$ *and evidence of direct CP violation in* $B \to K^*\pi$ *decays*, *Phys. Rev. D* **83** (2011) 112010 [arXiv:1105.0125] [INSPIRE].

[39] T. Skwarnicki, *A study of the radiative CASCADE transitions between the Upsilon-Prime and Upsilon resonances*, Ph.D. thesis, INP, Cracow, Poland (1986) [INSPIRE].

[40] ARGUS collaboration, *Search for hadronic* $b \to u$ *decays*, *Phys. Lett. B* **241** (1990) 278 [INSPIRE].

The LHCb collaboration

R. Aaij[38], A.S.W. Abdelmotteleb[57], C. Abellan Beteta[51], F. Abudinén[57], T. Ackernley[61], A. A. Adefisoye[69], B. Adeva[47], M. Adinolfi[55], P. Adlarson[84], C. Agapopoulou[14], C.A. Aidala[86], Z. Ajaltouni[11], S. Akar[11], K. Akiba[38], P. Albicocco[28], J. Albrecht[19,f], F. Alessio[49], Z. Aliouche[63], P. Alvarez Cartelle[56], R. Amalric[16], S. Amato[3], J.L. Amey[55], Y. Amhis[14], L. An[6], L. Anderlini[27], M. Andersson[51], P. Andreola[51], M. Andreotti[26], S. Andres Estrada[83], A. Anelli[31,o,49], D. Ao[7], F. Archilli[37,v], Z Areg[69], M. Argenton[26], S. Arguedas Cuendis[9,49], A. Artamonov[44], M. Artuso[69], E. Aslanides[13], R. Ataíde Da Silva[50], M. Atzeni[65], B. Audurier[12], J. A. Authier[15], D. Bacher[64], I. Bachiller Perea[50], S. Bachmann[22], M. Bachmayer[50], J.J. Back[57], P. Baladron Rodriguez[47], V. Balagura[15], A. Balboni[26], W. Baldini[26], L. Balzani[19], H. Bao[7], J. Baptista de Souza Leite[61], C. Barbero Pretel[47,12], M. Barbetti[27], I. R. Barbosa[70], R.J. Barlow[63], M. Barnyakov[25], S. Barsuk[14], W. Barter[59], J. Bartz[69], S. Bashir[40], B. Batsukh[5], P. B. Battista[14], A. Bay[50], A. Beck[65], M. Becker[19], F. Bedeschi[35], I.B. Bediaga[2], N. A. Behling[19], S. Belin[47], K. Belous[44], I. Belov[29], I. Belyaev[36], G. Benane[13], G. Bencivenni[28], E. Ben-Haim[16], A. Berezhnoy[44], R. Bernet[51], S. Bernet Andres[46], A. Bertolin[33], C. Betancourt[51], F. Betti[59], J. Bex[56], Ia. Bezshyiko[51], O. Bezshyyko[85], J. Bhom[41], M.S. Bieker[18], N.V. Biesuz[26], P. Billoir[16], A. Biolchini[38], M. Birch[62], F.C.R. Bishop[10], A. Bitadze[63], A. Bizzeti[27,p], T. Blake[57,b], F. Blanc[50], J.E. Blank[19], S. Blusk[69], V. Bocharnikov[44], J.A. Boelhauve[19], O. Boente Garcia[15], T. Boettcher[68], A. Bohare[59], A. Boldyrev[44], C.S. Bolognani[81], R. Bolzonella[26,l], R. B. Bonacci[1], N. Bondar[44,49], A. Bordelius[49], F. Borgato[33,49], S. Borghi[63], M. Borsato[31,o], J.T. Borsuk[82], E. Bottalico[61], S.A. Bouchiba[50], M. Bovill[64], T.J.V. Bowcock[61], A. Boyer[49], C. Bozzi[26], J. D. Brandenburg[87], A. Brea Rodriguez[50], N. Breer[19], J. Brodzicka[41], A. Brossa Gonzalo[47,†], J. Brown[61], D. Brundu[32], E. Buchanan[59], L. Buonincontri[33,q], M. Burgos Marcos[81], A.T. Burke[63], C. Burr[49], J.S. Butter[56], J. Buytaert[49], W. Byczynski[49], S. Cadeddu[32], H. Cai[74], Y. Cai[5], A. Caillet[16], R. Calabrese[26,l], S. Calderon Ramirez[9], L. Calefice[45], S. Cali[28], M. Calvi[31,o], M. Calvo Gomez[46], P. Camargo Magalhaes[2,aa], J. I. Cambon Bouzas[47], P. Campana[28], D.H. Campora Perez[81], A.F. Campoverde Quezada[7], S. Capelli[31], L. Capriotti[26], R. Caravaca-Mora[9], A. Carbone[25,j], L. Carcedo Salgado[47], R. Cardinale[29,m], A. Cardini[32], P. Carniti[31], L. Carus[22], A. Casais Vidal[65], R. Caspary[22], G. Casse[61], M. Cattaneo[49], G. Cavallero[26], V. Cavallini[26,l], S. Celani[22], S. Cesare[30,n], A.J. Chadwick[61], I. Chahrour[86], H. Chang[4,c], M. Charles[16], Ph. Charpentier[49], E. Chatzianagnostou[38], R. Cheaib[78], M. Chefdeville[10], C. Chen[56], J. Chen[50], S. Chen[5], Z. Chen[7], M. Cherif[12], A. Chernov[41], S. Chernyshenko[53], X. Chiotopoulos[81], V. Chobanova[83], M. Chrzaszcz[41], A. Chubykin[44], V. Chulikov[28,36], P. Ciambrone[28], X. Cid Vidal[47], G. Ciezarek[49], P. Cifra[38], P.E.L. Clarke[59], M. Clemencic[49], H.V. Cliff[56], J. Closier[49], C. Cocha Toapaxi[22], V. Coco[49], J. Cogan[13], E. Cogneras[11], L. Cojocariu[43], S. Collaviti[50], P. Collins[49], T. Colombo[49], M. Colonna[19], A. Comerma-Montells[45], L. Congedo[24], J. Connaughton[57], A. Contu[32], N. Cooke[60], C. Coronel[66], I. Corredoira [12], A. Correia[16], G. Corti[49], J. Cottee Meldrum[55], B. Couturier[49], D.C. Craik[51], M. Cruz Torres[2,g], E. Curras Rivera[50], R. Currie[59], C.L. Da Silva[68], S. Dadabaev[44], L. Dai[71], X. Dai[4], E. Dall'Occo[49], J. Dalseno[83], C. D'Ambrosio[62], J. Daniel[11], P. d'Argent[24], G. Darze[3], A. Davidson[57], J.E. Davies[63], O. De Aguiar Francisco[63], C. De Angelis[32,k], F. De Benedetti[49], J. de Boer[38], K. De Bruyn[80], S. De Capua[63], M. De Cian[63], U. De Freitas Carneiro Da Graca[2,a], E. De Lucia[28], J.M. De Miranda[2], L. De Paula[3], M. De Serio[24,h], P. De Simone[28], F. De Vellis[19], J.A. de Vries[81], F. Debernardis[24], D. Decamp[10], S. Dekkers[1], L. Del Buono[16], B. Delaney[65], H.-P. Dembinski[19], J. Deng[8], V. Denysenko[51], O. Deschamps[11], F. Dettori[32,k], B. Dey[78], P. Di Nezza[28], I. Diachkov[44], S. Didenko[44], S. Ding[69], Y. Ding[50], L. Dittmann[22], V. Dobishuk[53], A. D. Docheva[60], A. Doheny[57], C. Dong[4,c], A.M. Donohoe[23], F. Dordei[32], A.C. dos Reis[2], A. D. Dowling[69], L. Dreyfus[13], W. Duan[72], P. Duda[82], M.W. Dudek[41], L. Dufour[49], V. Duk[34], P. Durante[49], M. M. Duras[82], J.M. Durham[68], O. D. Durmus[78], A. Dziurda[41], A. Dzyuba[44], S. Easo[58], E. Eckstein[18], U. Egede[1], A. Egorychev[44], V. Egorychev[44], S. Eisenhardt[59], E. Ejopu[63], L. Eklund[84], M. Elashri[66], J. Ellbracht[19], S. Ely[62], A. Ene[43], J. Eschle[69], S. Esen[22], T. Evans[38], F. Fabiano[32], S. Faghih[66], L.N. Falcao[2], B. Fang[7], R. Fantechi[35], L. Fantini[34,r], M. Faria[50], K. Farmer[59], D. Fazzini[31,o], L. Felkowski[82], M. Feng[5,7], M. Feo[19], A. Fernandez Casani[48], M. Fernandez Gomez[47], A.D. Fernez[67], F. Ferrari[25,j], F. Ferreira Rodrigues[3], M. Ferrillo[51], M. Ferro-Luzzi[49], S. Filippov[44], R.A. Fini[24], M. Fiorini[26,l], M. Firlej[40], K.L. Fischer[64], D.S. Fitzgerald[86], C. Fitzpatrick[63], T. Fiutowski[40], F. Fleuret[15], A. Fomin[52], M. Fontana[25], L. F. Foreman[63], R. Forty[49], D. Foulds-Holt[59], V. Franco Lima[3], M. Franco Sevilla[67], M. Frank[49], E. Franzoso[26,l], G. Frau[63], C. Frei[49], D.A. Friday[63], J. Fu[7], Q. Führing[19,f,56], T. Fulghesu[13], G. Galati[24], M.D. Galati[38], A. Gallas Torreira[47], D. Galli[25,j], S. Gambetta[59], M. Gandelman[3], P. Gandini[30], B. Ganie[63], H. Gao[7], R. Gao[64], T.Q. Gao[56], Y. Gao[8], Y. Gao[6], Y. Gao[8], L.M. Garcia Martin[50], P. Garcia Moreno[45], J. García Pardiñas[65], P. Gardner[67], K. G. Garg[8], L. Garrido[45], C. Gaspar[49], A. Gavrikov[33], G. Gazzoni[11], L.L. Gerken[19], E. Gersabeck[20], M. Gersabeck[20], T. Gershon[57], S. Ghizzo[29,m], Z. Ghorbanimoghaddam[55], L. Giambastiani[33,q], F. I. Giasemis[16,e], V. Gibson[56], H.K. Giemza[42], A.L. Gilman[64], M. Giovannetti[28], A. Gioventù[45], L. Girardey[63,58], M.A. Giza[41], F.C. Glaser[14,22], V.V. Gligorov[16], C. Göbel[70], L. Golinka-Bezshyyko[85], E. Golobardes[46], D. Golubkov[44], A. Golutvin[62,49], S. Gomez Fernandez[45], W. Gomulka[40], I. Gonçales Vaz[49], F. Goncalves Abrantes[64], M. Goncerz[41], G. Gong[4,c], J. A. Gooding[19], I.V. Gorelov[44], C. Gotti[31], E. Govorkova[65], J.P. Grabowski[18], L.A. Granado Cardoso[49], E. Graugés[45], E. Graverini[50,t], L. Grazette[57], G. Graziani[27], A. T. Grecu[43], L.M. Greeven[38], N.A. Grieser[66], L. Grillo[60], S. Gromov[44], C. Gu[15], M. Guarise[26], L. Guerry[11], V. Guliaeva[44], P. A. Günther[22], A.-K. Guseinov[50], E. Gushchin[44], Y. Guz[6,49], T. Gys[49], K. Habermann[18], T. Hadavizadeh[1], C. Hadjivasiliou[67], G. Haefeli[50], C. Haen[49], S. Haken[56], G. Hallett[57], P.M. Hamilton[67], J. Hammerich[61], Q. Han[33], X. Han[22,49], S. Hansmann-Menzemer[22], L. Hao[7], N. Harnew[64], T. H. Harris[1], M. Hartmann[14], S. Hashmi[40], J. He[7,d], A. Hedes[63], F. Hemmer[49], C. Henderson[66], R. Henderson[14], R.D.L. Henderson[1], A.M. Hennequin[49], K. Hennessy[61], L. Henry[50], J. Herd[62], P. Herrero Gascon[22], J. Heuel[17], A. Hicheur[3], G. Hijano Mendizabal[51], J. Horswill[63],

JHEP12(2025)151

R. Hou[8], Y. Hou[11], D. C. Houston[60], N. Howarth[61], J. Hu[72], W. Hu[7], X. Hu[4,c], W. Hulsbergen[38], R.J. Hunter[57], M. Hushchyn[44], D. Hutchcroft[61], M. Idzik[40], D. Ilin[44], P. Ilten[66], A. Iniukhin[44], A. Ishteev[44], K. Ivshin[44], H. Jage[17], S.J. Jaimes Elles[76,49,48], S. Jakobsen[49], E. Jans[38], B.K. Jashal[48], A. Jawahery[67], C. Jayaweera[54], V. Jevtic[19], Z. Jia[16], E. Jiang[67], X. Jiang[5,7], Y. Jiang[7], Y. J. Jiang[6], E. Jimenez Moya[9], N. Jindal[87], M. John[64], A. John Rubesh Rajan[23], D. Johnson[54], C.R. Jones[56], S. Joshi[42], B. Jost[49], J. Juan Castella[56], N. Jurik[49], I. Juszczak[41], D. Kaminaris[50], S. Kandybei[52], M. Kane[59], Y. Kang[4,c], C. Kar[11], M. Karacson[49], A. Kauniskangas[50], J.W. Kautz[66], M.K. Kazanecki[41], F. Keizer[49], M. Kenzie[56], T. Ketel[38], B. Khanji[69], A. Kharisova[44], S. Kholodenko[35,49], G. Khreich[14], T. Kirn[17], V.S. Kirsebom[31,o], O. Kitouni[65], S. Klaver[39], N. Kleijne[35,s], K. Klimaszewski[42], M.R. Kmiec[42], S. Koliiev[53], L. Kolk[19], A. Konoplyannikov[6], P. Kopciewicz[49], P. Koppenburg[38], A. Korchin[52], M. Korolev[44], I. Kostiuk[38], O. Kot[53], S. Kotriakhova, E. Kowalczyk[67], A. Kozachuk[44], P. Kravchenko[44], L. Kravchuk[44], M. Kreps[57], P. Krokovny[44], W. Krupa[69], W. Krzemien[42], O. Kshyvanskyi[53], S. Kubis[82], M. Kucharczyk[41], V. Kudryavtsev[44], E. Kulikova[44], A. Kupsc[84], V. Kushnir[52], B. Kutsenko[13], I. Kyryllin[52], D. Lacarrere[49], P. Laguarta Gonzalez[45], A. Lai[32], A. Lampis[32], D. Lancierini[62], C. Landesa Gomez[47], J.J. Lane[1], G. Lanfranchi[28], C. Langenbruch[22], J. Langer[19], O. Lantwin[44], T. Latham[57], F. Lazzari[35,t,49], C. Lazzeroni[54], R. Le Gac[13], H. Lee[61], R. Lefèvre[11], A. Leflat[44], S. Legotin[44], M. Lehuraux[57], E. Lemos Cid[49], O. Leroy[13], T. Lesiak[41], E. D. Lesser[49], B. Leverington[22], A. Li[4,c], C. Li[4], C. Li[13], H. Li[72], J. Li[8], K. Li[75], L. Li[63], M. Li[8], P. Li[7], P.-R. Li[73], Q. Li[5,7], T. Li[71], T. Li[72], Y. Li[8], Y. Li[5], Y. Li[4], Z. Lian[4,c], Q. Liang[8], X. Liang[69], S. Libralon[48], A. L. Lightbody[12], C. Lin[7], T. Lin[58], R. Lindner[49], H. Linton[62], R. Litvinov[32], D. Liu[8], F. L. Liu[1], G. Liu[72], K. Liu[73], S. Liu[5,7], W. Liu[8], Y. Liu[59], Y. Liu[73], Y. L. Liu[62], G. Loachamin Ordonez[70], A. Lobo Salvia[45], A. Loi[32], T. Long[56], J.H. Lopes[3], A. Lopez Huertas[45], C. Lopez Iribarnegaray[47], S. López Soliño[47], Q. Lu[15], C. Lucarelli[49], D. Lucchesi[33,q], M. Lucio Martinez[48], Y. Luo[6], A. Lupato[33,i], E. Luppi[26,l], K. Lynch[23], X.-R. Lyu[7], G. M. Ma[4,c], S. Maccolini[19], F. Machefert[14], F. Maciuc[43], B. Mack[69], I. Mackay[64], L. M. Mackey[69], L.R. Madhan Mohan[56], M. J. Madurai[54], D. Magdalinski[38], D. Maisuzenko[44], J.J. Malczewski[41], S. Malde[64], L. Malentacca[49], A. Malinin[44], T. Maltsev[44], G. Manca[32,k], G. Mancinelli[13], C. Mancuso[14], R. Manera Escalero[45], F. M. Manganella[37], D. Manuzzi[25], D. Marangotto[30,n], J.F. Marchand[10], R. Marchevski[50], U. Marconi[25], E. Mariani[16], S. Mariani[49], C. Marin Benito[45], J. Marks[22], A.M. Marshall[55], L. Martel[64], G. Martelli[34], G. Martellotti[36], L. Martinazzoli[49], M. Martinelli[31,o], D. Martinez Gomez[80], D. Martinez Santos[83], F. Martinez Vidal[48], A. Martorell i Granollers[46], A. Massafferri[2], R. Matev[49], A. Mathad[49], V. Matiunin[44], C. Matteuzzi[69], K.R. Mattioli[15], A. Mauri[62], E. Maurice[15], J. Mauricio[45], P. Mayencourt[50], J. Mazorra de Cos[48], M. Mazurek[42], M. McCann[62], T.H. McGrath[63], N.T. McHugh[60], A. McNab[63], R. McNulty[23], B. Meadows[66], G. Meier[19], D. Melnychuk[42], D. Mendoza Granada[16], F. M. Meng[4,c], M. Merk[38,81], A. Merli[50,30], L. Meyer Garcia[67], D. Miao[5,7], H. Miao[7], M. Mikhasenko[77], D.A. Milanes[76,y], A. Minotti[31,o], E. Minucci[28], T. Miralles[11], B. Mitreska[19], D.S. Mitzel[19], A. Modak[58],

JHEP12(2025)151

L. Moeser[19], R.D. Moise[17], E. F. Molina Cardenas[86], T. Mombächer[49], M. Monk[57,1], S. Monteil[11], A. Morcillo Gomez[47], G. Morello[28], M.J. Morello[35,s], M.P. Morgenthaler[22], J. Moron[40], W. Morren[38], A.B. Morris[49], A.G. Morris[13], R. Mountain[69], H. Mu[4,c], Z. M. Mu[6], E. Muhammad[57], F. Muheim[59], M. Mulder[80], K. Müller[51], F. Muñoz-Rojas[9], R. Murta[62], V. Mytrochenko[52], P. Naik[61], T. Nakada[50], R. Nandakumar[58], T. Nanut[49], I. Nasteva[3], M. Needham[59], E. Nekrasova[44], N. Neri[30,n], S. Neubert[18], N. Neufeld[49], P. Neustroev[44], J. Nicolini[49], D. Nicotra[81], E.M. Niel[15], N. Nikitin[44], Q. Niu[73], P. Nogarolli[3], P. Nogga[18], C. Normand[55], J. Novoa Fernandez[47], G. Nowak[66], C. Nunez[86], H. N. Nur[60], A. Oblakowska-Mucha[40], V. Obraztsov[44], T. Oeser[17], A. Okhotnikov[44], O. Okhrimenko[53], R. Oldeman[32,k], F. Oliva[59,49], E. Olivart Pino[45], M. Olocco[19], C.J.G. Onderwater[81], R.H. O'Neil[49], J.S. Ordonez Soto[11], D. Osthues[19], J.M. Otalora Goicochea[3], P. Owen[51], A. Oyanguren[48], O. Ozcelik[49], F. Paciolla[35,w], A. Padee[42], K.O. Padeken[18], B. Pagare[47], T. Pajero[49], A. Palano[24], M. Palutan[28], C. Pan[74], X. Pan[4,c], S. Panebianco[12], G. Panshin[5], L. Paolucci[57], A. Papanestis[58], M. Pappagallo[24,h], L.L. Pappalardo[26], C. Pappenheimer[66], C. Parkes[63], D. Parmar[77], B. Passalacqua[26,l], G. Passaleva[27], D. Passaro[35,s,49], A. Pastore[24], M. Patel[62], J. Patoc[64], C. Patrignani[25,j], A. Paul[69], C.J. Pawley[81], A. Pellegrino[38], J. Peng[5,7], X. Peng[73], M. Pepe Altarelli[28], S. Perazzini[25], D. Pereima[44], H. Pereira Da Costa[68], M. Pereira Martinez[47], A. Pereiro Castro[47], C. Perez[46], P. Perret[11], A. Perrevoort[80], A. Perro[49,13], M.J. Peters[66], K. Petridis[55], A. Petrolini[29,m], J. P. Pfaller[66], H. Pham[69], L. Pica[35,s], M. Piccini[34], L. Piccolo[32], B. Pietrzyk[10], G. Pietrzyk[14], R. N. Pilato[61], D. Pinci[36], F. Pisani[49], M. Pizzichemi[31,o,49], V. M. Placinta[43], M. Plo Casasus[47], T. Poeschl[49], F. Polci[16], M. Poli Lener[28], A. Poluektov[13], N. Polukhina[44], I. Polyakov[63], E. Polycarpo[3], S. Ponce[49], D. Popov[7,49], S. Poslavskii[44], K. Prasanth[59], C. Prouve[83], D. Provenzano[32,k,49], V. Pugatch[53], G. Punzi[35,t], S. Qasim[51], Q. Q. Qian[6], W. Qian[7], N. Qin[4,c], S. Qu[4,c], R. Quagliani[49], B. Quintana[10], R.I. Rabadan Trejo[57], J.H. Rademacker[55], M. Rama[35], M. Ramírez García[86], V. Ramos De Oliveira[70], M. Ramos Pernas[57], M.S. Rangel[3], F. Ratnikov[44], G. Raven[39], M. Rebollo De Miguel[48], F. Redi[30,i], J. Reich[55], F. Reiss[20], Z. Ren[7], P.K. Resmi[64], M. Ribalda Galvez[45], R. Ribatti[50], G. Ricart[15,12], D. Riccardi[35,s], S. Ricciardi[58], K. Richardson[65], M. Richardson-Slipper[56], K. Rinnert[61], P. Robbe[14,49], G. Robertson[60], E. Rodrigues[61], A. Rodriguez Alvarez[45], E. Rodriguez Fernandez[47], J.A. Rodriguez Lopez[76], E. Rodriguez Rodriguez[49], J. Roensch[19], A. Rogachev[44], A. Rogovskiy[58], D.L. Rolf[19], P. Roloff[49], V. Romanovskiy[66], A. Romero Vidal[47], G. Romolini[26,49], F. Ronchetti[50], T. Rong[6], M. Rotondo[28], S. R. Roy[22], M.S. Rudolph[69], M. Ruiz Diaz[22], R.A. Ruiz Fernandez[47], J. Ruiz Vidal[81], J. J. Saavedra-Arias[9], J.J. Saborido Silva[47], S. E. R. Sacha Emile R.[49], R. Sadek[15], N. Sagidova[44], D. Sahoo[78], N. Sahoo[54], B. Saitta[32,k], M. Salomoni[31,49,o], I. Sanderswood[48], R. Santacesaria[36], C. Santamarina Rios[47], M. Santimaria[28], L. Santoro[2], E. Santovetti[37], A. Saputi, D. Saranin[44], A. Sarnatskiy[80], G. Sarpis[49], M. Sarpis[79], C. Satriano[36,u], M. Saur[73], D. Savrina[44], H. Sazak[17], F. Sborzacchi[49,28], A. Scarabotto[19], S. Schael[17], S. Scherl[61], M. Schiller[22], H. Schindler[49], M. Schmelling[21], B. Schmidt[49], S. Schmitt[17], H. Schmitz[18], O. Schneider[50], A. Schopper[62], N. Schulte[19],

JHEP12(2025)151

M.H. Schune[14], G. Schwering[17], B. Sciascia[28], A. Sciuccati[49], I. Segal[77], S. Sellam[47], A. Semennikov[44], T. Senger[51], M. Senghi Soares[39], A. Sergi[29,m], N. Serra[51], L. Sestini[27], A. Seuthe[19], B. Sevilla Sanjuan[46], Y. Shang[6], D.M. Shangase[86], M. Shapkin[44], R. S. Sharma[69], I. Shchemerov[44], L. Shchutska[50], T. Shears[61], L. Shekhtman[44], Z. Shen[38], S. Sheng[5,7], V. Shevchenko[44], B. Shi[7], Q. Shi[7], W. S. Shi[72], Y. Shimizu[14], E. Shmanin[25], R. Shorkin[44], J.D. Shupperd[69], R. Silva Coutinho[69], G. Simi[33,q], S. Simone[24,h], M. Singha[78], N. Skidmore[57], T. Skwarnicki[69], M.W. Slater[54], E. Smith[65], K. Smith[68], M. Smith[62], L. Soares Lavra[59], M.D. Sokoloff[66], F.J.P. Soler[60], A. Solomin[55], A. Solovev[44], N. S. Sommerfeld[18], R. Song[1], Y. Song[50], Y. Song[4,c], Y. S. Song[6], F.L. Souza De Almeida[69], B. Souza De Paula[3], E. Spadaro Norella[29,m], E. Spedicato[25], J.G. Speer[19], P. Spradlin[60], V. Sriskaran[49], F. Stagni[49], M. Stahl[77], S. Stahl[49], S. Stanislaus[64], M. Stefaniak[87], E.N. Stein[49], O. Steinkamp[51], H. Stevens[19], D. Strekalina[44], Y. Su[7], F. Suljik[64], J. Sun[32], J. Sun[63], L. Sun[74], D. Sundfeld[2], W. Sutcliffe[51], K. Swientek[40], F. Swystun[56], A. Szabelski[42], T. Szumlak[40], Y. Tan[4,c], Y. Tang[74], Y. T. Tang[7], M.D. Tat[22], J. A. Teijeiro Jimenez[47], A. Terentev[44], F. Terzuoli[35,w], F. Teubert[49], E. Thomas[49], D.J.D. Thompson[54], A. R. Thomson-Strong[59], H. Tilquin[62], V. Tisserand[11], S. T'Jampens[10], M. Tobin[5], T. T. Todorov[20], L. Tomassetti[26,l], G. Tonani[30], X. Tong[6], T. Tork[30], D. Torres Machado[2], L. Toscano[19], D.Y. Tou[4,c], C. Trippl[46], G. Tuci[22], N. Tuning[38], L.H. Uecker[22], A. Ukleja[40], D.J. Unverzagt[22], A. Upadhyay[49], B. Urbach[59], A. Usachov[39], A. Ustyuzhanin[44], U. Uwer[22], V. Vagnoni[25], V. Valcarce Cadenas[47], G. Valenti[25], N. Valls Canudas[49], J. van Eldik[49], H. Van Hecke[68], E. van Herwijnen[62], C.B. Van Hulse[47,z], R. Van Laak[50], M. van Veghel[38], G. Vasquez[51], R. Vazquez Gomez[45], P. Vazquez Regueiro[47], C. Vázquez Sierra[83], S. Vecchi[26], J.J. Velthuis[55], M. Veltri[27,x], A. Venkateswaran[50], M. Verdoglia[32], M. Vesterinen[57], W. Vetens[69], D. Vico Benet[64], P. Vidrier Villalba[45], M. Vieites Diaz[47], X. Vilasis-Cardona[46], E. Vilella Figueras[61], A. Villa[25], P. Vincent[16], B. Vivacqua[3], F.C. Volle[54], D. vom Bruch[13], N. Voropaev[44], K. Vos[81], C. Vrahas[59], J. Wagner[19], J. Walsh[35], E.J. Walton[1,57], G. Wan[6], A. Wang[7], B. Wang[5], C. Wang[22], G. Wang[8], H. Wang[73], J. Wang[6], J. Wang[5], J. Wang[4,c], J. Wang[74], M. Wang[49], N. W. Wang[7], R. Wang[55], X. Wang[8], X. Wang[72], X. W. Wang[62], Y. Wang[75], Y. Wang[6], Y. W. Wang[73], Z. Wang[14], Z. Wang[4,c], Z. Wang[30], J.A. Ward[57], M. Waterlaat[49], N.K. Watson[54], D. Websdale[62], Y. Wei[6], J. Wendel[83], B.D.C. Westhenry[55], C. White[56], M. Whitehead[60], E. Whiter[54], A.R. Wiederhold[63], D. Wiedner[19], M. A. Wiegertjes[38], C. Wild[64], G. Wilkinson[64,49], M.K. Wilkinson[66], M. Williams[65], M. J. Williams[49], M.R.J. Williams[59], R. Williams[56], S. Williams[55], Z. Williams[55], F.F. Wilson[58], M. Winn[12], W. Wislicki[42], M. Witek[41], L. Witola[19], T. Wolf[22], E. Wood[56], G. Wormser[14], S.A. Wotton[56], H. Wu[69], J. Wu[8], X. Wu[74], Y. Wu[6,56], Z. Wu[7], K. Wyllie[49], S. Xian[72], Z. Xiang[5], Y. Xie[8], T. X. Xing[30], A. Xu[35,s], L. Xu[4,c], L. Xu[4,c], M. Xu[49], Z. Xu[49], Z. Xu[7], Z. Xu[5], K. Yang[62], X. Yang[6], Y. Yang[15], Z. Yang[6], V. Yeroshenko[14], H. Yeung[63], H. Yin[8], X. Yin[7], C. Y. Yu[6], J. Yu[71], X. Yuan[5], Y Yuan[5,7], E. Zaffaroni[50], M. Zavertyaev[21], M. Zdybal[41], F. Zenesini[25], C. Zeng[5,7], M. Zeng[4,c], C. Zhang[6], D. Zhang[8], J. Zhang[7], L. Zhang[4,c], R. Zhang[8], S. Zhang[71], S. Zhang[64], Y. Zhang[6], Y. Z. Zhang[4,c], Z. Zhang[4,c],

JHEP12(2025)151

Y. Zhao [22], A. Zhelezov [22], S. Z. Zheng [6], X. Z. Zheng [4,c], Y. Zheng [7], T. Zhou [6], X. Zhou [8], Y. Zhou [7], V. Zhovkovska [57], L. Z. Zhu [7], X. Zhu [4,c], X. Zhu [8], Y. Zhu [17], V. Zhukov [17], J. Zhuo [48], Q. Zou [5,7], D. Zuliani [33,q], G. Zunica [50]

[1] *School of Physics and Astronomy, Monash University, Melbourne, Australia*
[2] *Centro Brasileiro de Pesquisas Físicas (CBPF), Rio de Janeiro, Brazil*
[3] *Universidade Federal do Rio de Janeiro (UFRJ), Rio de Janeiro, Brazil*
[4] *Department of Engineering Physics, Tsinghua University, Beijing, China*
[5] *Institute Of High Energy Physics (IHEP), Beijing, China*
[6] *School of Physics State Key Laboratory of Nuclear Physics and Technology, Peking University, Beijing, China*
[7] *University of Chinese Academy of Sciences, Beijing, China*
[8] *Institute of Particle Physics, Central China Normal University, Wuhan, Hubei, China*
[9] *Consejo Nacional de Rectores (CONARE), San Jose, Costa Rica*
[10] *Université Savoie Mont Blanc, CNRS, IN2P3-LAPP, Annecy, France*
[11] *Université Clermont Auvergne, CNRS/IN2P3, LPC, Clermont-Ferrand, France*
[12] *Université Paris-Saclay, Centre d'Etudes de Saclay (CEA), IRFU, Saclay, France, Gif-Sur-Yvette, France*
[13] *Aix Marseille Univ, CNRS/IN2P3, CPPM, Marseille, France*
[14] *Université Paris-Saclay, CNRS/IN2P3, IJCLab, Orsay, France*
[15] *Laboratoire Leprince-Ringuet, CNRS/IN2P3, Ecole Polytechnique, Institut Polytechnique de Paris, Palaiseau, France*
[16] *LPNHE, Sorbonne Université, Paris Diderot Sorbonne Paris Cité, CNRS/IN2P3, Paris, France*
[17] *I. Physikalisches Institut, RWTH Aachen University, Aachen, Germany*
[18] *Universität Bonn — Helmholtz-Institut für Strahlen und Kernphysik, Bonn, Germany*
[19] *Fakultät Physik, Technische Universität Dortmund, Dortmund, Germany*
[20] *Physikalisches Institut, Albert-Ludwigs-Universität Freiburg, Freiburg, Germany*
[21] *Max-Planck-Institut für Kernphysik (MPIK), Heidelberg, Germany*
[22] *Physikalisches Institut, Ruprecht-Karls-Universität Heidelberg, Heidelberg, Germany*
[23] *School of Physics, University College Dublin, Dublin, Ireland*
[24] *INFN Sezione di Bari, Bari, Italy*
[25] *INFN Sezione di Bologna, Bologna, Italy*
[26] *INFN Sezione di Ferrara, Ferrara, Italy*
[27] *INFN Sezione di Firenze, Firenze, Italy*
[28] *INFN Laboratori Nazionali di Frascati, Frascati, Italy*
[29] *INFN Sezione di Genova, Genova, Italy*
[30] *INFN Sezione di Milano, Milano, Italy*
[31] *INFN Sezione di Milano-Bicocca, Milano, Italy*
[32] *INFN Sezione di Cagliari, Monserrato, Italy*
[33] *INFN Sezione di Padova, Padova, Italy*
[34] *INFN Sezione di Perugia, Perugia, Italy*
[35] *INFN Sezione di Pisa, Pisa, Italy*
[36] *INFN Sezione di Roma La Sapienza, Roma, Italy*
[37] *INFN Sezione di Roma Tor Vergata, Roma, Italy*
[38] *Nikhef National Institute for Subatomic Physics, Amsterdam, Netherlands*
[39] *Nikhef National Institute for Subatomic Physics and VU University Amsterdam, Amsterdam, Netherlands*
[40] *AGH — University of Krakow, Faculty of Physics and Applied Computer Science, Kraków, Poland*
[41] *Henryk Niewodniczanski Institute of Nuclear Physics Polish Academy of Sciences, Kraków, Poland*
[42] *National Center for Nuclear Research (NCBJ), Warsaw, Poland*
[43] *Horia Hulubei National Institute of Physics and Nuclear Engineering, Bucharest-Magurele, Romania*
[44] *Authors affiliated with an institute formerly covered by a cooperation agreement with CERN.*
[45] *ICCUB, Universitat de Barcelona, Barcelona, Spain*
[46] *La Salle, Universitat Ramon Llull, Barcelona, Spain*

JHEP12(2025)151

[47] Instituto Galego de Física de Altas Enerxías (IGFAE), Universidade de Santiago de Compostela, Santiago de Compostela, Spain
[48] Instituto de Fisica Corpuscular, Centro Mixto Universidad de Valencia — CSIC, Valencia, Spain
[49] European Organization for Nuclear Research (CERN), Geneva, Switzerland
[50] Institute of Physics, Ecole Polytechnique Fédérale de Lausanne (EPFL), Lausanne, Switzerland
[51] Physik-Institut, Universität Zürich, Zürich, Switzerland
[52] NSC Kharkiv Institute of Physics and Technology (NSC KIPT), Kharkiv, Ukraine
[53] Institute for Nuclear Research of the National Academy of Sciences (KINR), Kyiv, Ukraine
[54] School of Physics and Astronomy, University of Birmingham, Birmingham, United Kingdom
[55] H.H. Wills Physics Laboratory, University of Bristol, Bristol, United Kingdom
[56] Cavendish Laboratory, University of Cambridge, Cambridge, United Kingdom
[57] Department of Physics, University of Warwick, Coventry, United Kingdom
[58] STFC Rutherford Appleton Laboratory, Didcot, United Kingdom
[59] School of Physics and Astronomy, University of Edinburgh, Edinburgh, United Kingdom
[60] School of Physics and Astronomy, University of Glasgow, Glasgow, United Kingdom
[61] Oliver Lodge Laboratory, University of Liverpool, Liverpool, United Kingdom
[62] Imperial College London, London, United Kingdom
[63] Department of Physics and Astronomy, University of Manchester, Manchester, United Kingdom
[64] Department of Physics, University of Oxford, Oxford, United Kingdom
[65] Massachusetts Institute of Technology, Cambridge, MA, United States
[66] University of Cincinnati, Cincinnati, OH, United States
[67] University of Maryland, College Park, MD, United States
[68] Los Alamos National Laboratory (LANL), Los Alamos, NM, United States
[69] Syracuse University, Syracuse, NY, United States
[70] Pontifícia Universidade Católica do Rio de Janeiro (PUC-Rio), Rio de Janeiro, Brazil, associated to [3]
[71] School of Physics and Electronics, Hunan University, Changsha City, China, associated to [8]
[72] Guangdong Provincial Key Laboratory of Nuclear Science, Guangdong-Hong Kong Joint Laboratory of Quantum Matter, Institute of Quantum Matter, South China Normal University, Guangzhou, China, associated to [4]
[73] Lanzhou University, Lanzhou, China, associated to [5]
[74] School of Physics and Technology, Wuhan University, Wuhan, China, associated to [4]
[75] Henan Normal University, Xinxiang, China, associated to [8]
[76] Departamento de Fisica, Universidad Nacional de Colombia, Bogota, Colombia, associated to [16]
[77] Ruhr Universitaet Bochum, Fakultaet f. Physik und Astronomie, Bochum, Germany, associated to [19]
[78] Eotvos Lorand University, Budapest, Hungary, associated to [49]
[79] Faculty of Physics, Vilnius University, Vilnius, Lithuania, associated to [20]
[80] Van Swinderen Institute, University of Groningen, Groningen, Netherlands, associated to [38]
[81] Universiteit Maastricht, Maastricht, Netherlands, associated to [38]
[82] Tadeusz Kosciuszko Cracow University of Technology, Cracow, Poland, associated to [41]
[83] Universidade da Coruña, A Coruña, Spain, associated to [46]
[84] Department of Physics and Astronomy, Uppsala University, Uppsala, Sweden, associated to [60]
[85] Taras Schevchenko University of Kyiv, Faculty of Physics, Kyiv, Ukraine, associated to [14]
[86] University of Michigan, Ann Arbor, MI, United States, associated to [69]
[87] Ohio State University, Columbus, United States, associated to [68]

[a] Centro Federal de Educacão Tecnológica Celso Suckow da Fonseca, Rio De Janeiro, Brazil
[b] Department of Physics and Astronomy, University of Victoria, Victoria, Canada
[c] Center for High Energy Physics, Tsinghua University, Beijing, China
[d] Hangzhou Institute for Advanced Study, UCAS, Hangzhou, China
[e] LIP6, Sorbonne Université, Paris, France
[f] Lamarr Institute for Machine Learning and Artificial Intelligence, Dortmund, Germany
[g] Universidad Nacional Autónoma de Honduras, Tegucigalpa, Honduras
[h] Università di Bari, Bari, Italy

JHEP12(2025)151

[i] Università di Bergamo, Bergamo, Italy
[j] Università di Bologna, Bologna, Italy
[k] Università di Cagliari, Cagliari, Italy
[l] Università di Ferrara, Ferrara, Italy
[m] Università di Genova, Genova, Italy
[n] Università degli Studi di Milano, Milano, Italy
[o] Università degli Studi di Milano-Bicocca, Milano, Italy
[p] Università di Modena e Reggio Emilia, Modena, Italy
[q] Università di Padova, Padova, Italy
[r] Università di Perugia, Perugia, Italy
[s] Scuola Normale Superiore, Pisa, Italy
[t] Università di Pisa, Pisa, Italy
[u] Università della Basilicata, Potenza, Italy
[v] Università di Roma Tor Vergata, Roma, Italy
[w] Università di Siena, Siena, Italy
[x] Università di Urbino, Urbino, Italy
[y] Universidad de Ingeniería y Tecnología (UTEC), Lima, Peru
[z] Universidad de Alcalá, Alcalá de Henares, Spain
[aa] Facultad de Ciencias Fisicas, Madrid, Spain
[†] Deceased

JHEP12(2025)151